
PET of Cardiac Transgene Expression: Comparison of 2 Approaches Based on Herpesviral Thymidine Kinase Reporter Gene

Masao Miyagawa, MD, PhD¹; Martina Anton, PhD²; Roland Haubner, PhD¹; Marcus V. Simoes, MD, PhD¹; Christian Stadele, DVM^{2,3}; Wolf Erhardt, DVM²; Sybille Reder, MT¹; Terry Lehner, BSc¹; Bettina Wagner, DVM¹; Steffi Noll, PhD⁴; Bernhard Noll, PhD⁴; Michaela Grote, PhD⁴; Sanjiv S. Gambhir, MD⁵; Bernd Gansbacher, MD²; Markus Schwaiger, MD¹; and Frank M. Bengel, MD¹

¹Nuklearmedizinische Klinik und Poliklinik, Technische Universitat Munchen, Munich, Germany; ²Institut fur Experimentelle Onkologie und Therapieforschung, Technische Universitat Munchen, Munich, Germany; ³Medizinische Klinik I, Technische Universitat Munchen, Munich, Germany; ⁴Institute for Bioinorganic and Radiopharmaceutical Chemistry, Forschungszentrum Rossendorf, Germany; and ⁵Department of Radiology and Bio-X Program, Stanford University, Stanford, California

PET of reporter gene expression holds promise for noninvasive monitoring of gene therapy. Previously, 2 approaches based on the herpes simplex virus type 1 thymidine kinase gene (HSV1-tk) have been successfully applied to the heart. Wild-type HSV1-tk was imaged with ¹²⁴I-labeled 2'-fluoro-2'-deoxy-5-iodo-1-β-D-arabinofuranosyl-5-iodouracil (FIAU), and a mutant HSV1-tk (HSV1-sr39tk) was imaged with ¹⁸F-labeled 9-[4-fluoro-3-(hydroxymethyl)butyl]guanine (FHBG). The aim of this study was to compare these 2 combinations with regard to specificity, imaging contrast, and reporter probe kinetics using dynamic PET in small and large animals. **Methods:** Similar titers of adenovirus-expressing wild-type HSV1-tk (Ad_{tk}), mutant HSV1-sr39tk (Ad_{sr39tk}), or control genes were directly injected into the myocardium of 24 rats and 8 pigs. Two days later, dynamic PET was performed with a clinical scanner during the 120 min after injection of ¹²⁴I-FIAU (Ad_{tk} animals and controls) or ¹⁸F-FHBG (Ad_{sr39tk} animals and controls). Imaging with ¹³N-ammonia was performed to identify cardiac regions of interest. **Results:** In rats, significant cardiac ¹²⁴I-FIAU accumulation occurred in images obtained early (10–30 min) after Ad_{tk} injection. Because of tracer washout, however, no difference between Ad_{tk}-injected animals and controls was seen in the images obtained later. For ¹⁸F-FHBG, specific myocardial accumulation greater than background levels was detected in Ad_{sr39tk}-injected animals at early imaging and, in contrast to ¹²⁴I-FIAU accumulation, increased over time until the latest imaging (105–120 min). At maximum, cardiac ¹⁸F-FHBG concentration showed a 4.15 ± 1.65-fold increase compared with controls (105–120 min), and cardiac ¹²⁴I-FIAU concentration reached a maximal increase of 1.34 ± 0.38-fold compared with controls (10–30 min, *P* = 0.0014). Global cardiac reporter probe kinetics in rats were confirmed by regional myocardial analysis in pig hearts. Transgene expression was specifically visualized by both approaches. The highest target-to-background ratio of ¹²⁴I-FIAU in Ad_{tk}-infected pig

myocardium was 1.50 ± 0.20, versus 2.64 ± 0.49 for ¹⁸F-FHBG in Ad_{sr39tk}-infected areas (*P* = 0.01). In vivo results were confirmed by ex vivo counting and autoradiography. **Conclusion:** Both reporter gene/probe combinations were feasible for noninvasive imaging of cardiac transgene expression in different species. Specific probe kinetics suggest different myocardial handling of pyrimidine (FIAU) and acycloguanosine (FHBG) derivatives. The results favor ¹⁸F-FHBG with mutant HSV1-sr39tk because of continuous accumulation over time and higher imaging contrast.

Key Words: gene therapy; reporter genes; HSV1-tk; reporter probes

J Nucl Med 2004; 45:1917–1923

Innovative approaches for cardiovascular molecular therapy are rapidly evolving, and translational efforts from experimental to clinical application are increasing. Gene and cell therapy hold great promise for treatment of heart disease, but despite progress, some basic principles are still under development (1,2). Examples of such open issues are the optimal method for delivery, therapeutic efficacy, the time course and magnitude of gene expression, and the fate of transplanted cells in target and remote areas. The use of reporter genes and radiolabeled reporter probes provides methodology to address these questions noninvasively. Reporter genes can be overexpressed together with therapeutic genes or within transplanted cells, and radionuclide imaging will allow for assessment of the location, magnitude, and persistence of transgene expression in the heart and the whole body (3–6).

Using PET, 2 approaches have been applied for cardiac reporter gene imaging. Both are based on the herpes simplex virus type 1 thymidine kinase gene (HSV1-tk). Using the pyrimidine derivative ¹²⁴I-labeled 2'-fluoro-2'-deoxy-5-iodo-1-β-D-arabinofuranosyl-5-iodouracil (FIAU) as re-

Received Mar. 9, 2004; revision accepted May 20, 2004.
For correspondence or reprints contact: Frank M. Bengel, MD, Nuklearmedizinische Klinik und Poliklinik, Technische Universitat Munchen, Klinikum rechts der Isar, Ismaninger Strasse 22, 81675 Munchen, Germany.
E-mail: frank.bengel@lrz.tum.de

porter probe, we recently reported that imaging of wild-type HSV1-tk expression after adenoviral gene transfer in pig hearts is feasible with a clinical PET scanner (6). But in contrast to studies on tumors (7–10), washout of ^{124}I -FIAU from the cardiac area of HSV1-tk expression was found to be a limitation for imaging at later times after injection.

In vivo images were also obtained using the acycloguanosine derivative ^{18}F -labeled 9-[4-fluoro-3-(hydroxymethyl)butyl]guanine (FHBG) and dedicated small-animal PET to identify expression of a mutant herpes HSV1-tk (HSV1-sr39tk) in rats after direct myocardial gene transfer or injection of transfected cells (3,5). ^{18}F -FHBG kinetics in the heart have not been evaluated to date, and potential differences in myocardial uptake and turnover of pyrimidine and acycloguanosine derivatives remain undetermined. The aim of this study was to apply and compare the 2 available reporter gene/reporter probe combinations for cardiac PET in small and large experimental animals.

MATERIALS AND METHODS

Adenoviral Vectors

Replication-defective type 5 adenoviral vectors, which carried either wild-type HSV1-tk (Ad_{tk}) or mutant HSV1-sr39tk ($\text{Ad}_{\text{sr39tk}}$) under transcriptional control of human cytomegalovirus early gene promoter, were constructed and purified as described previously (11,12). Vectors that carried either LacZ gene (Ad_{LacZ}) or no exogenous gene (Ad_{Null}) were used as negative controls (11). Double cesium chloride-purified vectors were used throughout the study, and titers were determined by plaque assay on 293 cells (13).

Radiolabeled Probes

^{124}I -FIAU was synthesized and purified as previously described (7). With ^{124}I -FIAU, overall radiochemical yield was approximately 70% and radiochemical purity was >98%. ^{18}F -FHBG was synthesized as developed at Forschungszentrum Rossendorf. Briefly, tosylated and methoxytritylated precursor was radiolabeled using K- ^{18}F -F/Kryptofix 2.2.2 (Merck) complex, and then protection groups were split off under acidic conditions. The labeling product was purified by high-performance liquid chromatography (HPLC). Radiochemical yield was 5%–15% (decay corrected) after 85–95 min of synthesis. Radiochemical purity was >98%, and average specific activity was 19 GBq/ μmol at the end of synthesis.

Rat Protocol

Experimental protocols were approved by the regional governmental commission of animal protection (Regierung von Oberbayern).

Under anesthesia (intramuscular midazolam, medetomidine, and fentanyl), 36 male Wistar rats (268 ± 23 g) received a percutaneous intramyocardial injection into the left ventricular inferior wall from the epigastric angle under echocardiographic guidance (14). Blue dye was injected into 12 animals, which were sacrificed immediately afterward. In short-axis slices (40 μm) of the excised hearts of all animals, the stained area, comprising $14\% \pm 4\%$ of the left ventricular circumference, was identified, hence demonstrating the reliability and reproducibility of the technique. Subsequently, 2.5×10^9 plaque-forming units (pfu) of

either Ad_{tk} ($n = 7$) or Ad_{LacZ} ($n = 7$) in a 200- μL volume were injected, followed by ^{124}I -FIAU PET 2 d later. In another series, 2.5×10^9 pfu of either $\text{Ad}_{\text{sr39tk}}$ ($n = 5$) or Ad_{LacZ} ($n = 5$) in a 200- μL volume were injected, followed by ^{18}F -FHBG PET 2 d later. After PET, the animals were sacrificed. Their hearts were rapidly removed, weighed, frozen, and analyzed ex vivo.

Pig Protocol

Eight young domestic pigs (20–30 kg) underwent left thoracotomy under anesthesia (isoflurane, 0.4–1.5 vol%; intravenous propofol, 7–10 mL/h; intravenous fentanyl as required). Genes were transferred by regional injection of 1×10^{10} pfu of adenovirus into the anterior myocardium. In 5 animals that were part of a previous study (6), Ad_{tk} or Ad_{Null} was injected, followed by ^{124}I -FIAU PET 2 d later. In 3 animals, $\text{Ad}_{\text{sr39tk}}$ and Ad_{Null} were injected in separate areas of basal and apical anterior wall, followed by ^{18}F -FHBG PET 2 d later. After in vivo PET, the animals were sacrificed. Their hearts were excised, rinsed, and sliced macroscopically into 5 short-axis slices, which were imaged ex vivo.

PET

All PET studies were performed using an ECAT EXACT HR + clinical scanner (CTI/Siemens). This scanner provides an axial field of view of 15.8 cm, resulting in 47 transverse slices with a slice separation of 3.4 mm. Supine 10-min transmission scans were obtained using ^{68}Ge rod sources. Then, ^{13}N -ammonia images (50–74 MBq for rats, 200–250 MBq for pigs) were obtained for 20 min to assess myocardial localization and perfusion. After a 30-min break to allow for radioactivity decay, a bolus of ^{124}I -FIAU or ^{18}F -FHBG (18–22 MBq for rats, 70–150 MBq for pigs) was injected intravenously, and dynamic imaging (six 10-min frames and four 15-min frames) was performed until 120 min after injection.

Rat Data Analysis. Emission data, corrected for random events, dead time, and attenuation, were reconstructed using an iterative reconstruction algorithm (ordered-subsets expectation maximization with 4 subsets and 8 iterations). The resulting in-plane resolution of axial images was 5 mm in full width at half maximum (7). Static ^{13}N -ammonia images were used to define circular, 1-cm-diameter regions of interest (ROIs) for the entire left ventricular myocardium on 6–7 transaxial slices. ROIs were copied to identical positions in ^{124}I -FIAU or ^{18}F -FHBG images. Then, the maximal pixels within ROIs in ^{124}I -FIAU or ^{18}F -FHBG images were depicted and maximal cardiac radionuclide concentrations were calculated and expressed as percentage dose per milliliter (= activity in the maximal pixel within ROIs [MBq/mL]/injected dose [MBq] $\times 100$) (8). Additionally, radioactivity concentrations for liver, thyroid, and stomach were determined.

Pig Data Analysis. Attenuation-corrected emission images were reconstructed by filtered backprojection. Volumetric sampling was performed to identify 460 myocardial segments in the perfusion study (15). Segments were then transferred to ^{124}I -FIAU or ^{18}F -FHBG images, and polar maps were generated. For regional analysis, a polar map of 9 myocardial areas was applied (anterior, lateral, septal, and inferior walls divided into basal and distal areas; apex as a separate area). Areas of Ad_{tk} , $\text{Ad}_{\text{sr39tk}}$, and Ad_{Null} injection, along with remote areas (inferior wall) were defined for each animal according to the experimental protocol. Then, circular ROIs were placed on transaxial images, using ^{13}N -ammonia images for guidance. Regional myocardial concentrations (percentage dose per milliliter) were estimated from maximum pixels

within ROIs. The count ratio of ^{124}I -FIAU or ^{18}F -FHBG relative to remote myocardium was calculated for each interval.

Plasma Metabolite Analysis. In pigs, venous blood was taken at 7, 30, and 120 min for metabolite analysis. Sample collection, preparation, and HPLC analysis for ^{124}I -FIAU were performed as previously described (6). For ^{18}F -FHBG, aliquots (350 μL) were injected onto a Multisphere 100 RP-18 column (5 μm ; 150 \times 10 mm; flow, 3 mL/min; CS-Chromatographie Service). The gradient was 0%–50% acetonitrile in water containing 0.1% trifluoroic acid over 20 min. Detection was performed using a flow scintillation analyzer (Radiomatic 500 TR Series; Packard Canberra Co.).

Ex Vivo Analysis

Rats. Radioactivity in each heart was measured by γ -counting. Results were expressed as percentage injected dose per gram of tissue. Then, 40- μm slices were prepared (HM500OM microtome; Microm) and digital autoradiography (PhosphorImager 445SI; Molecular Dynamics) was performed for all slices from an animal on the same imaging plate. Ratios of maximal counts in virus injection areas relative to remote area were calculated. LacZ gene expression was assessed by β -galactosidase staining in rats injected with Ad_{LacZ} to identify the virus injection site (9).

Pigs. Macroscopic cardiac short-axis slices were repositioned in the PET scanner. A 10-min transmission scan was obtained, followed by a 30-min emission scan. In attenuation-corrected images, ROIs were defined manually for 9 myocardial areas, similarly to in vivo analysis, and regional tracer concentration was calculated as a percentage of the average of all areas.

Statistical Analysis

Mean values are given with SD. Data were analyzed with JMP 4.0 software (SAS Institute Inc.). Differences were assessed by paired/unpaired t testing as appropriate. Simple linear regression was used to describe relationships between pairs of continuous variables. P values < 0.05 were considered statistically significant.

RESULTS

In Vivo Imaging in Rats

Cardiac Reporter Probe Kinetics. Figure 1 shows examples of whole-body images of reporter probe distribution early and late after injection, along with the time course of myocardial uptake. Significant cardiac ^{124}I -FIAU accumulation was seen in images obtained early after Ad_{tk} injection. Because of washout, no difference between Ad_{tk} -injected animals and controls was seen at later imaging. For ^{18}F -FHBG, specific myocardial accumulation greater than background levels was detected in $\text{Ad}_{\text{sr39tk}}$ -injected animals at early imaging and, in contrast to ^{124}I -FIAU accumulation, increased over time until the latest imaging. At maximum, cardiac ^{18}F -FHBG concentration showed a 4.15 ± 1.65 -fold increase compared with controls (105–120 min), and cardiac ^{124}I -FIAU concentration reached a maximal increase of 1.34 ± 0.38 -fold compared with controls (10–30 min; $P = 0.0014$).

Kinetics in Other Organs. Kinetics of radioactivity in extracardiac organs were also assessed (Fig. 2). Hepatic ^{124}I -FIAU accumulation was seen in early images but decreased over time. Furthermore, accumulation of radioactivity in thyroid and stomach increased with time in all animals. Differences between Ad_{tk} -injected animals and controls were not observed. For ^{18}F -FHBG, hepatic accumulation was pronounced in rats injected with $\text{Ad}_{\text{sr39tk}}$. A significant increase relative to controls with time after injection was observed.

Ex Vivo Validation. Postmortem analysis revealed a significant correlation between cardiac ^{124}I -FIAU or ^{18}F -FHBG accumulation estimated by PET and γ -counting of the heart

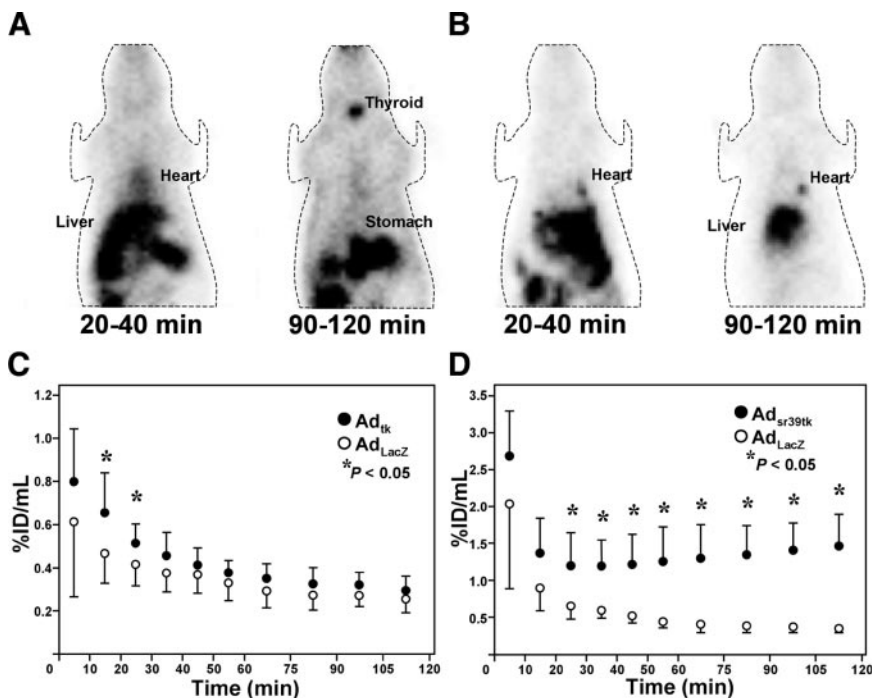


FIGURE 1. (A and B) PET coronal slices of representative rats at 20–40 min and at 90–120 min after intravenous injection of ^{124}I -FIAU (A) and ^{18}F -FHBG (B), obtained 2 d after intramyocardial injection of Ad_{tk} (A) or $\text{Ad}_{\text{sr39tk}}$ (B). (C and D) Cardiac tracer uptake over the entire 2 h after application of radiolabeled probes. Values are mean \pm SD in groups after intramyocardial injections with Ad_{tk} or negative control (Ad_{LacZ}) for ^{124}I -FIAU (C) and with $\text{Ad}_{\text{sr39tk}}$ or Ad_{LacZ} for ^{18}F -FHBG (D).

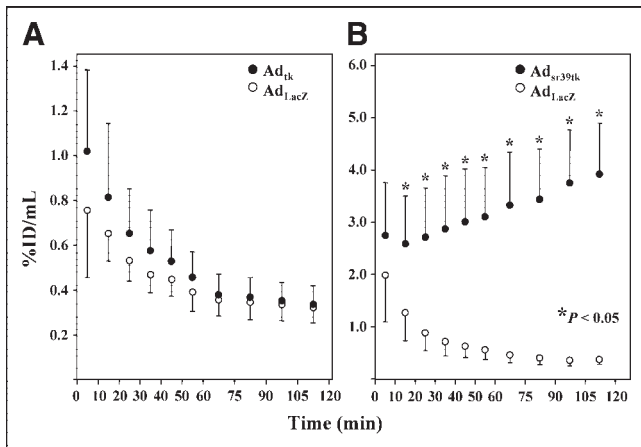


FIGURE 2. Kinetics of radiolabeled probes in the liver, ^{124}I -FIAU (A) and ^{18}F -FHBG (B). Values are mean \pm SD for each group.

($R = 0.789$, $P = 0.0008$ for ^{124}I -FIAU; $R = 0.852$, $P = 0.0017$ for ^{18}F -FHBG). Autoradiography demonstrated specific radioactivity accumulation in the regions of Ad_{tk} or $\text{Ad}_{\text{sr39tk}}$ injection. The count ratio of ^{124}I -FIAU relative to remote myocardium was 4.03 ± 1.94 in Ad_{tk} -injected areas, compared with 1.02 ± 0.30 for Ad_{LacZ} areas identified by β -galactosidase staining. The count ratio of ^{18}F -FHBG relative to remote myocardium was 10.08 ± 2.31 in $\text{Ad}_{\text{sr39tk}}$ areas, compared with 1.01 ± 0.11 for Ad_{LacZ} areas ($P = 0.0001$).

In Vivo Imaging in Pigs

Additional experiments were performed on pigs to evaluate interspecies reproducibility. Figure 3 shows representative myocardial images using both approaches and the time course of target-to-background ratios for areas transfected with reporter gene. Coregistered myocardial perfu-

sion was mildly heterogeneous in all animals after myocardial gene transfer, but no perfusion defects were observed.

^{124}I -FIAU/ Ad_{tk} . As previously reported, ^{124}I -FIAU uptake was seen to be significantly elevated in all myocardial areas infected with Ad_{tk} on images obtained 20–40 min after injection (6). HSV1-tk-expressing areas could no longer be distinguished from blood pool on images obtained 105–120 min after injection. No significant accumulation was observed in Ad_{Null} -infected areas or remote myocardium. The count ratio relative to remote myocardium was significantly higher for Ad_{tk} -infected areas than for Ad_{Null} areas during the first 30 min after injection. The highest count ratio relative to remote myocardium was 1.50 ± 0.20 for ^{124}I -FIAU at 20–30 min.

^{18}F -FHBG/ $\text{Ad}_{\text{sr39tk}}$. Early images showed ^{18}F -FHBG uptake to be significantly elevated in areas infected with $\text{Ad}_{\text{sr39tk}}$. In contrast to ^{124}I -FIAU, specific regional uptake continuously increased with time after injection. Starting 30 min after injection, the count ratio relative to remote myocardium was significantly higher than that relative to Ad_{Null} areas. The highest target-to-background ratio for ^{18}F -FHBG— 2.64 ± 0.49 at 105–120 min—was significantly higher than the highest ratio for ^{124}I -FIAU ($P = 0.01$).

Plasma Metabolites. Free iodine was seen for ^{124}I -FIAU and increased with time after injection but remained lower than the peak of labeled ^{124}I -FIAU, as previously described (6). The ratio of free iodine to labeled ^{124}I -FIAU was 0.22 ± 0.18 at 7 min, 0.39 ± 0.33 at 30 min, and 0.56 ± 0.13 at 120 min. Additional metabolites were not identified. For ^{18}F -FHBG, a peak of unidentified radiolabeled metabolite with a shorter retention time was present at HPLC in measurable amounts (about 30%) at 7 min and increased progressively to about 80% of total activity in plasma by 2 h. Activity in the ^{18}F -FHBG peak area divided by that in the total area under the radiochromatogram was $70\% \pm 1\%$ at 7 min,

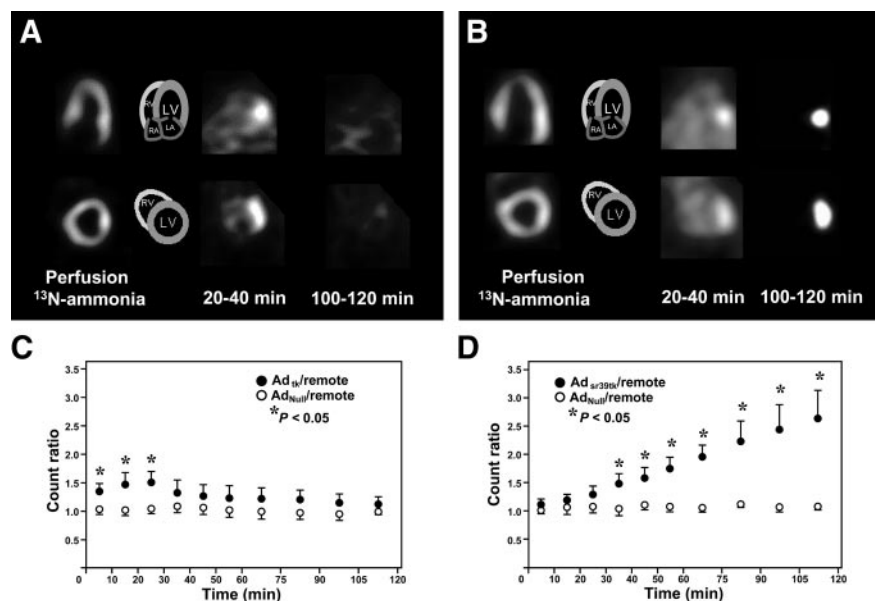


FIGURE 3. (A and B) PET slices of myocardial perfusion and early and late reporter probe distribution in pig hearts, 2 d after intramyocardial injection of Ad_{tk} (imaged by ^{124}I -FIAU) (A) or $\text{Ad}_{\text{sr39tk}}$ (imaged by ^{18}F -FHBG) (B) into basal anterolateral wall. Shown are representative horizontal long-axis slices (top) and short-axis slices (bottom). (C and D) Values for the count ratio of virus injection area relative to remote myocardium over the entire 2 h after application of radiolabeled probes. Values are mean \pm SD for ^{124}I -FIAU (C) and ^{18}F -FHBG (D). LA = left atrium; RA = right atrium; LV = left ventricle; RV = right ventricle.

23% \pm 4% at 30 min, and 19% \pm 4% at 120 min. The ratio of unidentified metabolite to ^{18}F -FHBG was 0.44 \pm 0.01 at 7 min, 3.4 \pm 0.4 at 30 min, and 4.3 \pm 0.7 at 120 min. No other peaks were detected, suggesting absence of further metabolites.

Ex Vivo Validation. PET of macroscopic heart slices revealed increased radioactivity in areas of Ad_{tk} or $\text{Ad}_{\text{sr39tk}}$ injection (Fig. 4). The segmental ex vivo ^{124}I -FIAU concentration correlated significantly with early myocardial in vivo ^{124}I -FIAU uptake ($R = 0.843$, $P < 0.0001$), whereas the segmental ex vivo ^{18}F -FHBG concentration correlated significantly with late myocardial in vivo ^{18}F -FHBG uptake ($R = 0.945$, $P < 0.0001$).

DISCUSSION

The usefulness of reporter genes and specific reporter probes for noninvasive imaging is increasingly emphasized because of the potential for in vivo monitoring of the location, magnitude, and persistence of transgene expression in target tissue. There has been considerable experience with nuclear imaging of HSV1-tk reporter gene expression in oncology (7–10,12,16,17). Radioiodinated ^{124}I -FIAU as a pyrimidine nucleoside derivative has preferentially been used for imaging wild-type HSV1-tk expression, whereas radiofluorinated ^{18}F -FHBG as an acycloguanosine derivative has been used for imaging mutant HSV1-sr39tk reporter gene expression. Recently, the usefulness of these techniques has been tested in the heart. A correlation between in vivo reporter probe accumulation and immunohistochemistry of reporter gene product has been demonstrated in both combinations (3–6). To date, several comparisons of these combinations have been performed on tumor cells, but the results conflicted (8,17). Furthermore, transfer of data obtained from tumors to the myocardial setting may be difficult because of different tissue metabolic properties, a

different susceptibility for adenoviral infection, and different proliferation rates.

Image Contrast and Reporter Probe Kinetics

We recently demonstrated in another study that infection of myocardial cells with $\text{Ad}_{\text{sr39tk}}$ or Ad_{tk} gives rise to comparable amounts of herpesviral thymidine kinase protein messenger RNA. Although the accumulation of ^{18}F -FHBG in vitro was only slightly higher in $\text{Ad}_{\text{sr39tk}}$ -infected cells than in Ad_{tk} -infected cells, we did detect considerably less accumulation of ^{14}C -FIAU in mutant TK-expressing cells in this previous project (18). These data supported in vivo use of Ad_{tk} as a preferable vector for FIAU imaging and of $\text{Ad}_{\text{sr39tk}}$ as a preferable vector for ^{18}F -FHBG. No further extensive experiments to describe kinetics in vitro were performed in this study, mainly because in vitro observations are difficult to transfer to the in vivo setting. In vivo kinetics are available, and those are of critical importance for practical application.

In vivo kinetics of the 2 reporter probes in this study differed significantly when similar amounts of vector were applied. In HSV1-tk-transfected hearts, specific ^{124}I -FIAU uptake was present only early after injection and decreased subsequently. This observation, which was previously reported for pig hearts (6), was reproducible in rat hearts. At later times after injection, specific tracer uptake was detectable no longer in vivo, but only ex vivo after removal of background activity. In contrast, the kinetics of ^{18}F -FHBG in hearts transfected with mutant HSV1-sr39tk showed a continuous increase of cardiac accumulation with time after injection. In the rats of this study, spatial resolution was limited because of acquisition with a clinical PET scanner. Thus, we also evaluated the myocardial kinetics of ^{18}F -FHBG in a large-animal model, pigs. Probe kinetics were reproducible across species and were associated with higher

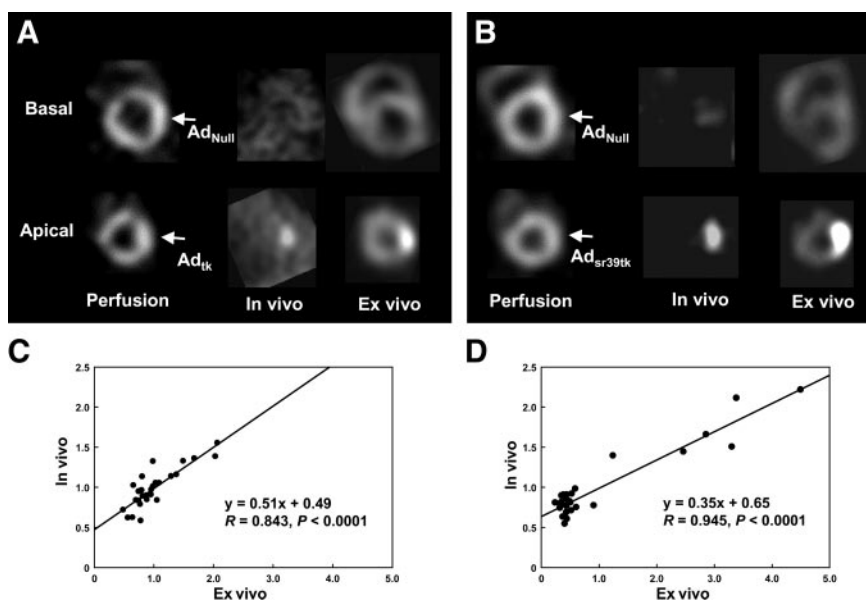


FIGURE 4. (A and B) Comparison of in vivo and ex vivo PET images of pig hearts. Shown are short-axis slices of a representative animal that was imaged using ^{124}I -FIAU after intramyocardial injection of Ad_{Null} into basal and Ad_{tk} into apical anterolateral walls (A) (arrows mark injection site) and of another animal that was imaged using ^{18}F -FHBG after injection of Ad_{Null} into basal and $\text{Ad}_{\text{sr39tk}}$ into apical anterolateral walls (B). (C and D) Correlation plots for segmental ex vivo tracer concentration in all animals and early myocardial in vivo ^{124}I -FIAU uptake (C) or late myocardial in vivo ^{18}F -FHBG uptake (D).

maximal target-to-background ratios and larger differences between animals expressing reporter gene and control animals.

Myocardial probe kinetics may be influenced by systemic degradation. Metabolite analysis of ^{124}I -FIAU demonstrated deiodination, consistent with previous studies (6,8). Plasma analysis after ^{18}F -FHBG injection in pigs also demonstrated the rapid appearance of a metabolite, which remains unknown but has been previously reported in monkeys, albeit in a smaller amount than we observed in pigs (19). Metabolite analysis of ^{18}F -FHBG has also been reported in humans (20). In our study, the amount of intact labeled reporter probe at the end of imaging was higher for ^{124}I -FIAU than for ^{18}F -FHBG. Thus, systemic degradation cannot explain the observed differences in myocardial kinetics, which have to be attributed to myocardium-specific mechanisms.

In tumors, ^{124}I -FIAU is thought to be taken up by cells, phosphorylated intracellularly by gene product, and then incorporated into host DNA (10). Owing to the lower tissue proliferation rates in myocardium than in tumors, DNA turnover and thus DNA incorporation of nucleotides (phosphorylated nucleosides) is expected to be low. This may facilitate intracellular degradation and tracer efflux. Speculatively, high myocardial expression of nucleotidase enzymes, which are responsible for production of adenosine as a vasoactive and cardioprotective agent, may facilitate intramyocardial dephosphorylation and thus washout of phosphorylated ^{124}I -FIAU (6), and phosphorylated ^{18}F -FHBG may not be a good substrate for these nucleotidase enzymes. To further refine understanding of the apparently complex kinetics of radiolabeled nucleoside reporter probes, detailed studies to dissect the processes of transport, phosphorylation, dephosphorylation, and DNA incorporation will be necessary along with identification and characterization of agents suitable for specific pharmacologic interventions.

Another strength of PET reporter gene imaging is that in addition to heart, other organs can be monitored—for example, to identify vector leakage to systemic circulation as a safety issue for gene therapy. Whole-body imaging of rats allowed for evaluating the feasibility of the 2 probes for this purpose. Gradually increased accumulation of radioactivity in thyroid and stomach after ^{124}I -FIAU injection is related to systemic deiodination and is not specific for reporter gene expression. In the liver as the primary target organ for systemically administered adenovirus in rats (21), the difference in ^{124}I -FIAU uptake between animals receiving intramyocardial injection of Ad_{tk} and animals receiving control virus did not reach statistical significance. In contrast, ^{18}F -FHBG liver uptake was pronounced and significantly higher in $\text{Ad}_{\text{sr39tk}}$ -injected rats than in controls. Because systemic vector contamination during intramyocardial injection and egress of adenovirus from the myocardium into systemic circulation are likely to occur in the rat model, ^{18}F -FHBG may be more sensitive than ^{124}I -FIAU for detecting extramyocardial vector leakage.

Practical Implications for Cardiac Reporter Gene Imaging

Although, in comparison with the oncologic setting, the cardiac setting still has only limited experience with in vivo imaging of gene expression, there is great potential for this technique in the monitoring of molecular therapies. Cardiac gene therapy can be evaluated by coexpressing reporter genes and therapeutic genes. Furthermore, reporter genes can be transferred to cells before transplantation for studies of cell trafficking, such as studies of cardiac stem cell therapy (5). The use of heart-specific promoters to drive reporter genes not only may provide tissue-specific readout but also may allow for linkage of the reporter signal to expression of specific endogenous genes in the future (22). This emphasizes the need to identify the most suitable reporter gene and reporter probe combination. Although advantages have been identified for ^{18}F -FHBG and mutant HSV1-sr39tk in this study, reporter genes other than HSV1-tk have been applied in the noncardiac setting. Some, such as dopamine D_2 receptor or sodium iodide symporter, have the advantage of producing a gene that lacks immunogenicity (23). Future studies will need to include these alternative approaches for evaluation and comparison to identify an optimal approach for reporter gene imaging of the heart in a given setting.

CONCLUSION

HSV1-tk–based reporter gene and reporter probe combinations are feasible for cardiac transgene expression. Specific reporter probe kinetics suggest different myocardial handling for pyrimidine and acycloguanosine derivatives. Results favor the combination of mutant HSV1-sr39tk reporter gene and ^{18}F -FHBG reporter probe because of continuous accumulation over time and the resultant higher contrast for PET. This approach may therefore be preferable for future monitoring of cardiac gene therapy or cell transplantation.

ACKNOWLEDGMENTS

The authors are indebted to Bryan Essien for assistance with vector preparation and to Wolfgang Linke for assistance with preparation of radiolabeled probes. This study was supported by grants from Deutsche Forschungsgemeinschaft (Be 2217/4-1); the Kommission für klinische Forschung, Klinikum rechts der Isar (KKF 8764167); and Fundação de Amparo à Pesquisa do Estado de São Paulo (01/04868-8).

REFERENCES

1. Isner JM. Myocardial gene therapy. *Nature*. 2002;415:234–239.
2. Forrester JS, Price MJ, Makkar RR. Stem cell repair of infarcted myocardium: an overview for clinicians. *Circulation*. 2003;108:1139–1145.
3. Wu JC, Inubushi M, Sundaresan G, Schelbert HR, Gambhir SS. Positron emission tomography imaging of cardiac reporter gene expression in living rats. *Circulation*. 2002;106:180–183.
4. Inubushi M, Wu JC, Gambhir SS, et al. Positron-emission tomography reporter gene expression imaging in rat myocardium. *Circulation*. 2003;107:326–332.

5. Wu JC, Chen IY, Sundaresan G, et al. Molecular imaging of cardiac cell transplantation in living animals using optical bioluminescence and positron emission tomography. *Circulation*. 2003;108:1302–1305.
6. Bengel FM, Anton M, Richter T, et al. Noninvasive imaging of transgene expression by use of positron emission tomography in a pig model of myocardial gene transfer. *Circulation*. 2003;108:2127–2133.
7. Brust P, Haubner R, Friedrich A, et al. Comparison of [¹⁸F]FHPG and [¹²⁴I/125I]FIAU for imaging herpes simplex virus type 1 thymidine kinase gene expression. *Eur J Nucl Med*. 2001;28:721–729.
8. Tjuvajev JG, Doubrovin M, Akhurst T, et al. Comparison of radiolabeled nucleoside probes (FIAU, FHBG, and FHPG) for PET imaging of HSV1-tk gene expression. *J Nucl Med*. 2002;43:1072–1083.
9. Jacobs A, Tjuvajev JG, Dubrovin M, et al. Positron emission tomography-based imaging of transgene expression mediated by replication-conditional, oncolytic herpes simplex virus type 1 mutant vectors in vivo. *Cancer Res*. 2001;61:2983–2995.
10. Haubner R, Avril N, Hantzopoulos PA, Gansbacher B, Schwaiger M. In vivo imaging of herpes simplex virus type 1 thymidine kinase gene expression: early kinetics of radiolabelled FIAU. *Eur J Nucl Med*. 2000;27:283–291.
11. Bengel FM, Anton M, Avril N, et al. Uptake of radiolabeled 2'-fluoro-2'-deoxy-5-iodo-1-β-D-arabinofuranosyluracil in cardiac cells after adenoviral transfer of the herpesvirus thymidine kinase gene: the cellular basis for cardiac gene imaging. *Circulation*. 2000;102:948–950.
12. Gambhir SS, Bauer E, Black ME, et al. A mutant herpes simplex virus type 1 thymidine kinase reporter gene shows improved sensitivity for imaging reporter gene expression with positron emission tomography. *Proc Natl Acad Sci USA*. 2000;97:2785–2790.
13. Hitt M, Bett AJ, et al. Techniques for human adenovirus vector construction and characterization. In: Adolph KW, ed. *Viral Gene Techniques*. San Diego, CA: Academic Press; 1995:13–30.
14. Weig HJ, Laugwitz KL, Moretti A, et al. Enhanced cardiac contractility after gene transfer of V2 vasopressin receptors in vivo by ultrasound-guided injection or transcatheter delivery. *Circulation*. 2000;101:1578–1585.
15. Nekolla SG, Miethaner C, Nguyen N, Ziegler SI, Schwaiger M. Reproducibility of polar map generation and assessment of defect severity and extent assessment in myocardial perfusion imaging using positron emission tomography. *Eur J Nucl Med*. 1998;25:1313–1321.
16. Tjuvajev JG, Stockhammer G, Desai R, et al. Imaging the expression of transfected genes in vivo. *Cancer Res*. 1995;55:6126–6132.
17. Min JJ, Iyer M, Gambhir SS. Comparison of [¹⁸F]FHBG and [¹⁴C]FIAU for imaging of HSV1-tk reporter gene expression: adenoviral infection vs stable transfection. *Eur J Nucl Med Mol Imaging*. 2003;30:1547–1560.
18. Anton M, Wittermann C, Haubner R, et al. Coexpression of herpesviral thymidine kinase reporter gene and VEGF gene for noninvasive monitoring of therapeutic gene transfer: an in vitro evaluation. *J Nucl Med*. 2004;45:1743–1746.
19. Alauddin MM, Shahinian A, Gordon EM, Bading JR, Conti PS. Preclinical evaluation of the penciclovir analog 9-(4-[¹⁸F]fluoro-3-hydroxymethylbutyl)guanine for in vivo measurement of suicide gene expression with PET. *J Nucl Med*. 2001;42:1682–1690.
20. Yaghoubi S, Barrio JR, Dahlbom M, et al. Human pharmacokinetic and dosimetry studies of [¹⁸F]FHBG: a reporter probe for imaging herpes simplex virus type-1 thymidine kinase reporter gene expression. *J Nucl Med*. 2001;42:1225–1234.
21. Guzman RJ, Lemarchand P, Crystal RG, Epstein SE, Finkel T. Efficient gene transfer into myocardium by direct injection of adenovirus vectors. *Circ Res*. 1993;73:1202–1207.
22. Franz WM, Rothmann T, Frey N, Katus HA. Analysis of tissue-specific gene delivery by recombinant adenoviruses containing cardiac-specific promoters. *Cardiovasc Res*. 1997;35:560–566.
23. Avril N, Bengel FM. Defining the success of cardiac gene therapy: how can nuclear imaging contribute? *Eur J Nucl Med Mol Imaging*. 2003;30:757–771.

